ISSN 0104-7760

Gokhan Gunduz[1], Mehmet Ali Oral[1], Mehmet Akyuz[2], Deniz Aydemir[1], Barbaros Yaman[1], Nejla Asik[1], Ali Savas Bulbul[3], Surhay Allahverdiyev[1]

PHYSICAL, MORPHOLOGICAL PROPERTIES AND RAMAN SPECTROSCOPY OF CHESTNUT BLIGHT DISEASED *CASTANEA SATIVA* MILL. WOOD

Keywords:
Cambium
Castanea sativa Mill.
Chestnut Blight
Raman Spectroscopy
SEM-EDX.

ABSTRACT: In this study, some of the physical and anatomical properties of Chestnut Blight Diseased (CBD) wood were investigated, and the study also included observations using Raman spectroscopy. The objective of these investigations was to determine the extent of the damage that is done to the wood of the diseased chestnut trees, which must be removed from the forest and used in the manufacture of industrial products. It was indicated that most of the adverse effects of the disease were in the vascular cambium. There was a clear indication of deterioration of the wood in the last growth ring next to vascular cambium. In the diseased secondary xylem region next to vascular cambium; vessel diameter, vessel frequency and vessel element length had a decrease, and vessel and other cells were irregular compared to healthy wood. Spores were detected and identified as *Cryphonectria parasitica* (Murrill). Annual ring properties (annual growth ring width, latewood percentage, etc.) were similar in diseased wood compared to healthy wood. The Raman spectroscopy results showed no significant changes in the structure of the cell wall or its components. After removing the diseased parts, unlimited usage of formerly wood is possible. Heat treatment of the wood is suggested before use in the interest of sanitation and dimensional stability.

Histórico:
Recebido 29/10/2015
Aceito 16/02/2016

PROPRIEDADES FÍSICAS E MORFOLÓGICAS E ESPECTROSCOPIA RAMAN DE MADEIRA DE *CASTANEA SATIVA* MILL. AFETADA PELO CANCRO DO CASTANHEIRO

Palavras chave:
Cambio
Castanea sativa Mill.
Cancro do castanheiro
Espectroscopia Ram
SEM-EDX

RESUMO: Neste estudo, algumas das propriedades físicas e anatômicas de madeira afetada pelo cancro do castanheiro (CBD) foram investigadas, e o estudo também incluiu observações usando espectroscopia Raman. O objetivo destas investigações foi determinar a dimensão do dano que é causado na madeira dos castanheiros doentes, que devem ser removidos da floresta e utilizados na fabricação de produtos industriais. Foi avaliado que a maioria dos efeitos adversos da doença esta localizado no câmbio vascular. Há uma clara indicação de deterioração da madeira no último anel de crescimento junto ao câmbio vascular. Na região doente do xilema secundário ao lado do câmbio vascular o diâmetro, frequência e comprimento do vaso eram menores, e os vasos e outras células eram irregulares comparados à madeira saudável. Esporos foram detectados e identificados como *Cryphonectria parasitica* (Murrill). Propriedades dos anéis anuais (largura de anéis de crescimento anual, porcentagem de lenho tardio, etc.) foram similares em madeira doente e madeira saudável. O resultado da espectroscopia Raman não mostrou mudança significativa na estrutura da parede celular ou dos seus componentes. Depois de retirar as partes doentes, o uso ilimitado da madeira é possível. Tratamento térmico da madeira é sugerido antes da utilização para fins de saneamento e estabilidade dimensional.

Correspondência:
gokhangunduz70@yahoo.com

DOI:
10.1590/01047760201622012101

[1] Bartin University - Bartin, Turkey
[2] Bulent Ecevit University - Zonguldak, Turkey

INTRODUCTION

Chestnut (*Castanea sativa* Mill.) trees are generally distributed in the southern part of Europe, East Asia, Europe, and eastern North America, and they have been an important resource due to their vital nutritional, cultural, and economic importance for thousands of years. Chestnut trees provide edible fruit and good-quality timber in many countries, including China, Turkey, Italy, and Korea (DOGU et al., 2011; METAXAS, 2013). The chestnut is produces in various countries (Table 1).

Dried chestnut wood has a high resistance to decay due to extractive compounds, such as tannins. Chestnut wood is used for many applications, such as the construction of buildings and wooden furniture, shipbuilding, timbers, and musical instruments. This important tree species was used extensively until the ocoruence of the fatal disease chestnut blight (CBD) caused by Cryphonectria parasitica (Murrill), which was first observed in the United States. In 1905, it was observed that American chestnut trees were dying in the Bronx Zoological Park in New York City (Anagnostakis 1987; Yazici 1998; Locci 2003; Jacobs 2007; Gündüz et al. 2011). Later, in 1938, the deadly fungus was observed for the first time in Europe, and it spread rapidly all over Italy and surrounding countries, becoming one of the major pathogens that attacked chestnut trees and leading to serious damage to European forests (Anagnostakis 1987; Robin and Heiniger 2001). Fig. 1 shows the history of the distribution of the disease in Europe.

In stationary growth, the fungus produces *in vitro* a large amount of an exopolysaccharide fraction that contains pullulan, a linear α-glucan β-D-galactan, and a galactomannan, all of which showed greater phytotoxic activity than that of the crude exopolysaccharide fraction (LOCCI, 2003; MOLINARO et al., 2000). The pathogen infects stem tissues and kills the above ground portions of trees by girdling the cambium. Chestnut blight cankers can be seen most easily on the bark of juvenile trees when their bark is wet. At that time, the orange color of the epidermis is usually obvious where the mycelium of the fungus has penetrated. Cankers are not easily seen on mature bark, where often the first sign of blight infection is the formation of the epitomic shoots below the canker. *Castanea dentata* has a ring-porous wood with larger early wood vessels formed in the spring. If the cambium is unable to make new vessels because it was killed by chestnut blight or some other injury, the tree forms shoots to bypass the blockage (ANAGNOSTAKIS, 1987; BARAKAT et al., 2012).

Many studies have been conducted in an effort to identify an approach or approaches that will stop and/or heal this disease. The simplest method to control the disease is removing the diseased branches of the diseased chestnut trees (FREINKEL, 2007). The hypo-virulent fungi strains in diseased chestnut woods also have been used as a biological control; this fungi is easy to identify because of its characteristic pathogenetic effect and the color of the mycelium (yellow in the virulent strains, white in the hypo-virulent strains) (ANAGNOSTAKIS, 1987, 2001; LOCCI, 2003).

Many studies have been conducted about the control with hypovirulent strains which is useful but requires extensive effort because every individual tree must be inoculated, and the inoculations are not 100% effective (ROBIN; HEINIGER, 2001). Schafleitner and Wilhelm (1997) indicated that chestnut trees diseased by hypovirulent strains survive due to their recognition and induction of defense mechanisms. Another potential method for preventing the disease is to increase the trees' natural resistance against the pathogen. Tests on forests and agricultural plants in Turkey, Russia, and Azerbaijan have been conducted using effective microorganisms (EM) to produce plants that are resistant to environmental biotic and abiotic stresses. It is known that chestnut trees start to fructify after 5-7 years, but sample tress treated with EM fructified after 3-4 years in the same conditions. The results showed

TABLE 1 Chestnut production by various countries (FOOD AND AGRICULTURE ORGANIZATION OF THE UNITED STATES - FAO, 2012).

Country	2006	2007	2008	2009	2010	2011	2012
China	1.139.660	1.266.510	1.450.450	1.550.000	1.620.000	1.600.000	1.650.000
Turkey	53.814	55.100	55.395	61.697	59.171	60.270	59.789
Italy	52.615	50.000	55.000	50.872	48.810	57.493	52.000
Korea	82.450	77.524	75.171	75.911	68.630	55.780	70.000
Bolivia	55.000	42.801	58.442	53.577	53.577	53.577	57.000
Others	108.400	102.951	94.537	94.454	99.697	87.616	81.328
Total	1.491.939	1.594.886	1.788.995	1.886.511	1.949.885	1.914.736	1.970.117

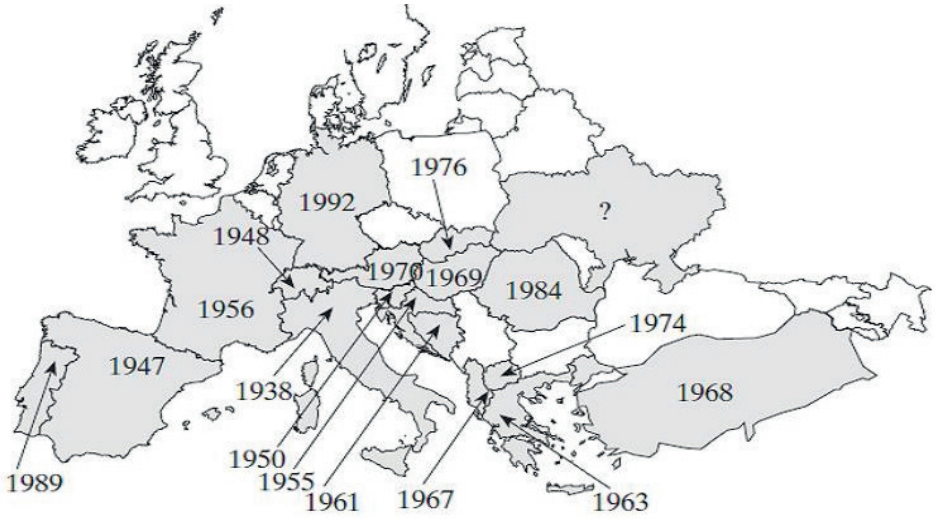

FIGURE 1 Distribution of chestnut blight disease in Europe (Robin and Heiniger 2001).

that EM technology can increase the productivity and resistance of chestnut trees (ALLAHVERDIYEV et al., 2011). Another study compared the bark extracts based on the inhibitory activity on fungal polygalacturonase and found Chinese chestnut bark extracts to be better inhibitors than American chestnut bark extracts. It also was found that a proteinaceous fraction of Chinese bark was a highly effective inhibitor of the same enzyme (HAVIR; ANAGNOSTAKIS, 1998). Defense-related genes with differential transcript abundance (GDTA) are candidates for host resistance to the chestnut blight fungus, *Cryphonectria parasitica* (Murrill). The salicylic acid (SA) pathway, which is considered one of the major pathways involved in the defense against nectrotrophic pathogens, regulates the expression of defense effector genes and systemic acquired resistance through the repression of the auxin signaling pathway. Abscissic acid (ABA) is another hormone that affects the resistance of chestnut trees against this disease. Other signaling genes involved in systemic acquired resistance (SAR), which is an effective defense mechanism against a broad range of pathogens and insects, induce numerous defense genes, include apoplastic lipid transfer protein and basic chitinase. Anti-fungal tests showed that proteins with a chitin binding domain, i.e., proteins C1, C3, and C4, inhibit hyphal growth of the chestnut blight fungus *Cryphonectria parasitica* (Murrill.) in culture (VANNINI et al., 1999;BARAKAT et al., 2012).

The reason and headway of the CBD are well known, and the main weights of the studies are about the CBD itself and the protection and cure of the disease. Diseased trees are removed from the diseased areas and used in various ways. Obviously, the anatomy and physical properties of the timber are factors in deciding how it will be used. There also is a lack of research about the detailed structure of the changes in the vascular cambium, secondary xylem and phloem as a result of the disease. The aim of this study was to determine and compare the anatomy and the physical properties of blight-diseased chestnut wood and healthy chestnut wood and their potential uses.

MATERIALS AND METHODS

Material

A single chestnut tree was chosen for use in this study in Bartin – Amasra forestry district (41°43'34.2"N 32°24'19.0"E) location. This decision was made because it was concluded that the comparison of the physical and anatomical changes in the healthy and diseased zones of the same tree would produce more statistically reliable results. Another reason to select a single sample tree is to eliminate genotypical differences in different individuals.

The sample tree was 15 m in height and 32 cm in diameter. The tests specimens were taken at 1.60 m height above the ground in the form of a disc that includes the infected area. The disc was cut into 2 x 2 x 3 cm sized samples to compare and to find out the long term effect of the disease. These samples covers all parts of the cross section (from bark to pith) and were prepared for a number of analyses, such as anatomical characterization by light microscopy (LM), scanning electron microscopy (SEM/EDX), Raman spectroscopy (RS), and physical properties, such as density, wood-water relations, bulk density, and macroscopic properties (Figure 2).

The long term annual (1954-2013) average temperature and participation of Bartin is 12.7 °C and 86.59 kg/m^2 respectively (MGM, 2014).

Methods

Determination of the Physical Properties

The evaluations of healthy and diseased wood were conducted according to relevant Turkish standards, such as: TS 53 Wood - Sampling and test methods - Determination of physical properties TS2471 Wood - Determination of Moisture Content for Physical and Mechanical Tests; TS2472 Wood - Determination of Density for Physical and Mechanical Tests; TS4083 Wood - Determination of Radial and Tangential Shrinkage; TS4084 Wood- Determination of Radial and Tangential Swelling; TS4085 Wood - Determination of Volumetric Shrinkage; TS4086 Wood- Determination of Volumetric Swelling (TURKISH STANDARTS, 1981a, 1981b, 1983a, 1983b, 1983c, 1983d, 1985).

Annual ring properties (sapwood and heartwood ratio, latewood percentage) also were measured by using stereomicroscopy, and the results were evaluated. All statistical analysis (Anova and Tukey Multiple Comparison Test) were made with StatgraphicsPlus software.

Determination of Anatomical Properties and Morphological Characterization

Both diseased and healthy wood samples with dimensions of 2 x 2 x 3 cm were taken from a diseased chestnut tree to determine the anatomical features of thin (20 μm) transverse, radial, and tangential sections. This was done by using a Eidg. Forschungsanstalt für Wald, Schnee und Landschaft (WSL) lightweight G.S.L.$^{-1}$ microtome for the light microscopical study of wood anatomy. All of the anatomical sections were prepared as recommended by Gaertner and Schweingruber (2013). To achieve statistically reliable results, the guidance provided by The International Association of Wood Anatomists Committee - IAWA Committee (1989) was used to determine the diameter, element length, and frequency of the vessels; the length, width, lumen width, and thickness of the cell wall of the fibers; and the width, height, and frequency of the rays. The vessel element and fiber length were measured on macerated wood (WISE et al., 1946).

Specimens of the fungi were taken to the laboratory and microscopically examined under Leica DM 750 digital imaging system Sections were hand cut using a razor blade. The fungi were identified using the relevant literature (Saccardo 1882; Saccardo 1905; Mel'nik 2000; Gruyter et al. 2010). Host plants were identified using the "Flora of Turkey and East Aegean Islands" (Davis 1982). Taxa, family, and author citations were listed according to (Cannon and Kirk 2007; Kirk et al. 2008), and fungal names according to Index Fungorum (www.speciesfungorum.org, accessed 2015).

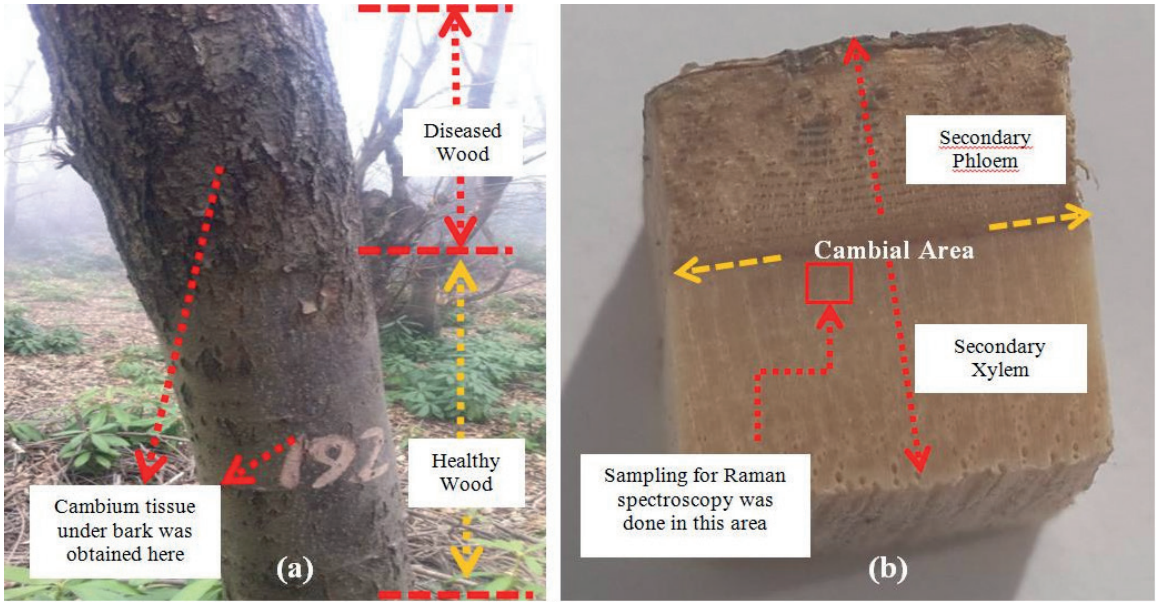

FIGURE 2 Samples used in the study: (a) appearance of the sample tree in the forest; (b) samples for microscopic (LM, SEM) and Raman spectroscopy investigation.

Raman Spectroscopy Preperation

Raman spectroscopy was conducted on the samples prepared for the light microscopy analysis. FT-Raman spectra of all samples were recorded with a RENISHAW inVia Raman Microscope between 300 and 3000 cm^{-1}. Grating 1200 l/mm, exposure time of 10 s. Laser power was between 0.3% (diseased wood) and 0.5 % (healthy wood) at a wavelength of 785 nm. The slit opening was 50 μm (centre 1672 μm).

For the morphological analysis, the healthy and diseased samples were observed after fracture of the samples under nitrogen with an environmental scanning electron microscope (ESEM) (FEI QUANTA FEG 450) with an accelerating voltage of 5 kV. The samples were coated with an Au film, and the SEM images were obtained using a secondary electron detector (ETD).

RESULTS AND DISCUSSION

Physical Properties

Data for variations on air-dried density ($\rho_{12\%}$), fully-dried density ($\rho_{0\%}$), cell wall material rate (CWR), and air space rate (ASR) (Table 2).

The data in Table 2 indicate that there was no difference in the fully-dried density values of the healthy and diseased samples, which were 0.56 and 0.55 $g \cdot cm^{-3}$, respectively, whereas the air-dried density was 0.59 $g \cdot cm^{-3}$ for the healthy samples and 0.64 $g \cdot cm^{-3}$ for the diseased samples. This result was found to be statistically significant. The variation of the density showed that the diseased wood absorbed less water than the healthy wood. The cell wall material ratio for the healthy wood and the diseased wood were both around 37%, and the air gap ratios for the healthy and diseased wood were both about 63%. The fiber saturation point, dimensional changes, and the density value in volume of the samples were shown in Table 3.

The density values in volume were determined to be 0.47 $g \cdot cm^{-3}$ for the healthy samples, whereas the diseased samples had a value of 0.50 $g \cdot cm^{-3}$; according to the variance analyses results, there was no statistically significant difference between these two groups. Shrinking and swelling values were determined as 10.2 and 11.3%, respectively, for the healthy samples and 9.6 and 11.1%, respectively, for the diseased samples. The small difference between the shrinking and swelling values of the two groups indicated why the diseased samples were denser. Thus, it can be said that this situation can be balanced while diseased wood contains less moisture. The highest water absorption of the wood was determined to be about 159% for the healthy samples and about 133% for the diseased wood, and this difference was statistically significant. The fiber saturation points for the healthy and diseased samples were about 22 and 19%, respectively. In light of these results, it can be said that the diseased wood contained less cellulose and hemicellulose because the components of the cells' walls contained fewer free OH^- groups, resulting in less water molecules binding to the cells. It is suggested that the decrease of the cellulose and hemicelluloses in the cell material resulted from *Cryphonectria parasitica* (Murrill) using cellulose and hemicelluloses as the carbon source for the development of its own colony.

TABLE 3 Fiber saturation point, dimensional changes, and the density value in volume of the samples.

			Healthy	Diseased
Fiber saturation point	n		7.00	9.00
	X		21.70	19.20
Tangential and radial swelling-α/ shrinkage-β	n	β	7.00	10.00
	X	α	7.00	7.00
	n	β	9.60	9.20
	X	α	11.10	10.50
Volumetric swelling-α / shrinkage-β	n	β	7.00	10.00
	X	α	7.00	7.00
	n	β	10.20	9.60
	X	α	11.30	11.10
The density value in volume	n		7.00	10.00
	X		0.47	0.50
Maximum Water Absorption (%)	X		159.30	132.90

TABLE 2 Air-dried and fully-dried density (ρ12% and ρ0%, respectively), cell wall material rate (CWR), and air space rate (ASR) values of the samples

	H1	H2	H3	H4	D1	D2	D3	D4	D5
n	73	69	81	109	41	60	79	81	123
ρ0%	0.56	0.55	0.56	0.55	0.55	0.55	0.55	0.55	0.55
ρ12%	0.56	0.58	0.60	0.60	0.66	0.63	0.65	0.64	0.62
HDO	37.57	37.07	37.18	37.08	37.54	36.59	36.18	36.85	36.81
HBO	62.43	62.93	62.82	62.91	62.46	63.41	63.82	63.15	63.19

Annual Ring Properties

Widths of the heartwood and sapwood, the number of annual rings of heartwood and sapwood, and the ratio of the diameter of the heartwood to the bark-free diameters of the healthy and diseased portions of the chestnut wood (Table 4).

Table 5 provides the annual ring widths, which is the one of the macroscopic properties of the wood, the correlation between the width of the annual rings of wood and the width of late wood, and the mean participation rate of late wood in the annual ring values of the healthy and diseased chestnut wood.

The relationship between the width of the annual rings and the late wood of the healthy and diseased portions of chestnut wood was determined by regression analysis. Accordingly, the regression coefficient of the healthy portion was found to be (r) = 0.955, which means this relationship was strong. As a result of the regression analysis of the diseased wood, the correlation coefficient was found to be (r) = 0.964, and this relationship also was strong. Both relationships, i.e., for diseased and healthy wood, were determined to be similar and significant.

Anatomical Properties

Table 6 and 7 provide the average values of the diameter and frequency of the vessels and the average values of width, height, and frequency of the rays.

In both the healthy and diseased parts of the chestnut wood, ring porosity was present, and the annual rings were distinct. The porosity and distinctness of the annual rings were not changed in the diseased wood. However, the tangential and radial diameters of the vessels were 181 – 260 μm in the earlywood of the diseased part and 195 – 274 μm in the earlywood of the healthy part. These diameters for the late wood were determined to be 42 –52 μm and 44 – 55 μm, respectively. The tangential and radial diameters of the vessels were smaller in the diseased wood than in the healthy wood. The average vessel frequency in the earlywood of the diseased and healthy parts were 5.7 and 5.9, respectively. The vessel frequency values in the latewood were determined to be 44 and 29, respectively. It can be seen that the number of vessels (vessel frequency) in the latewood was 34% lower than that in the healthy parts. The average width of the rays was found to be 18 μm, and there was no difference in this value between the healthy and diseased samples. However, the height of the rays and their frequency for the diseased woods were 246 μm and 8 units respectively, whereas they were 264 μm and 11 units respectively, for the healthy wood. These data indicate that there were fewer and lower rays in the diseased portions.

According to the measurements of the macerated wood, the lengths, widths, and wall thickness of the fibers and the lengths of the vessel elements have lower values in the diseased chestnut wood (Table 8). Figure 3 shows general views of the cells. In light of these values, it was concluded that the physiological and cambial activities of the diseased site of the chestnut tree were slowed by *Cryphonectria parasitica* (Murrill).

In general, there are no variations in the shapes of the vessel elements, but smaller vessel diameters and smaller vessel frequency were determined in the transverse section of the diseased wood. Moreover, the lengths of the vessel elements were shorter in the diseased part. When we examined the morphologies of the fiber cells, it was observed that the diseased wood's fibers had abnormal formation than those of the healthy wood. Also, bifurcations and different irregular structures

TABLE 5 Values related to the annual rings of healthy and diseased chestnut wood.

	Earlywood width (mm)	Latewood width (mm)	ARW (mm)	Latewood (%)
Healthy	1.056	4.531	5.587	80.004
Diseased	1.112	5.618	6.731	82.206

*Annual ring width (ARW) and Latewood %, relationship between annual rings and latewood width.

TABLE 6 Average values of the diameter and frequency of the vessel.

		Vessel Tangential Diameter (µm)	Vessel Radial Diameter (µm)	Vessel Frequency (Units)
Healthy	Earlywood	194.720	273.920	5.944
	Latewood	44.240	54.720	43.728
Diseased	Earlywood	181.144	260.720	5.768
	Latewood	42.480	52.400	28,704

TABLE 4 Heartwood and sapwood measurements and annual ring numbers of healthy and diseased portions of chestnut wood.

	Heartwood Thickness (cm)	Annual Ring in heartwood (units)	Sapwood Thickness (cm)	Annual ring in sapwood (units)	Heartwood ratio (%)
Healthy	6.12	12	2.82	4	68.46
Diseased	7.84	12	2.93	4	72.79

TABLE 7 Average values of the width, height, and frequency of the rays (N=250).

	Ray width (µm)	Ray height (µm)	Ray Frequency (Units)
Healthy	18	264	11
Diseased	18	246	8

were observed at the ends of the fibers of the diseased wood (Figure. 3).

The bifurcated ends of fibers might be a result of the increase of anticlinal divisions in the vascular cambium under stress conditions caused by the fungus. This phenomena can also be seen in compression wood in Gymnosperms as a result of developmental processes (anticlinal division and following it the intrusive growth) (TULIK, 2000).

This in turn, one may think, causes the surface of the diseased wood to become rougher, and this also may cause difficulty in processing the wood material. These formations are very limited and easy to remove, so they do not affect the economic value of the wood.

Morphological Characterization

SEM/EDX and LM on the cambium tissue

Light microscope images of the vascular cambium, secondary xylem and secondary phloem are indicating significant differences between diseased and healthy parts (Figure 4). While the images of the healthy parts had highly regular appearances, abnormalities can be observed in the shapes of the cells of the diseased parts. While cell walls can be clearly distinguished in the healthy parts, this is not true for the diseased parts. To support these findings, healthy and diseased parts were studied in detail by using an electron microscope, and the resulting SEM images are presented in Figure 5.

The SEM images showed the same irregularities in the diseased vascular cambium and secondary xylem. A silky and irregular appearance of the wood surface showed the clear difference in Figure 5 d and h.

In parallel to these changes, EDX analysis was conducted to whether there were different chemical substances in the structure of the healthy and diseased woods, Figure 9 and Figure. 10, respectively.

Different substances were determined in the EDX analysis done on the diseased vascular cambium. There was about 5% nitrogen in the vascular cambium according to the elemental analysis. Based on this result, it can be said that there is a chemical change in the vascular cambium in the diseased part.

SEM/EDX on the tangential direction of wood

Figure 6 shows various sizes of the parenchyma cells in the SEM images of the tangential sections of the diseased wood, and in some of the parenchyma cells, starch grains were observed. These grains only existed in some of the parenchyma cells. While only a single grain was determined in some parenchyma cells, others had 20-30 such grains. For better visualization, the SEM images of these grains are presented in Figure 7 a, b, e and f.

As a result of this observation, starch grains were observed in healthy and diseased wood. In addition, when the internal structure of the vessels were examined in tangential section, the surface was found to be smooth in healthy wood (Figure 7 g-h), while some granular formation was observed on the diseased wood (Figure 7e-d). It is likely that these structures resulted from the activity of the disease. Figure 8 shows the results of the elemental analyses of the starch grains that were conducted by SEM/EDX. The SEM/EDX analysis indicated that the structure of the starch grains was composed of carbon and oxygen.

Spore analysis

As a result of the analyses and other investigations, the chestnut wood fungus that caused this disease was determined to be *Cryphonectria parasitica* (Murrill) (Figure 9). According to the data that were acquired, the fungus penetrates into the wood through the spaces between the sections of bark, and then it causes changes, specifically in the vascular cambium, and in the fibers and vessels of the wood. The analysis of the fungus showed

TABLE 8 Average values of width, lumen width, length, and double cell wall thickness of the fibers and vessel element length (N=50).

	Vessel Element Length (µm)	Fiber length (µm)	Fiber width (µm)	Fiber lumen width (µm)	Fiber Double cell wall thickness (µm)
Healthy	588.000	1010.600	22.416	12.650	9.745
Diseased	423.800	823.600	21.606	11.992	9.614

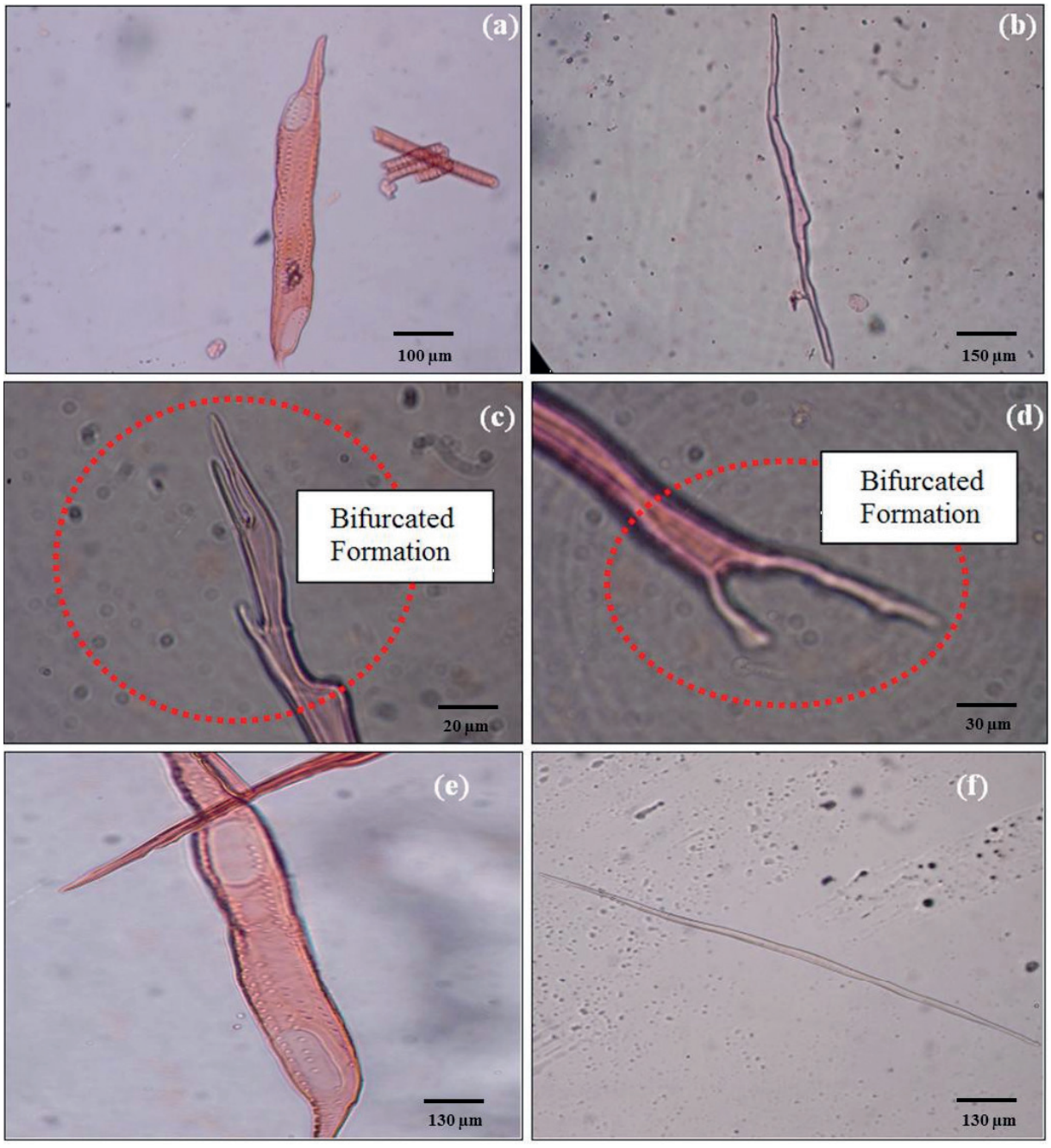

FIGURE 3 Fiber and vessel element of healthy and diseased wood: (a) vessel element of the diseased wood; b, c, d) bifurcated formations on the fibers of diseased wood and surface disturbances; (e) vessel element of the healthy wood; (f) healthy wood fiber (Light Microscopy).

that the formations were *Cryphonectria parasitica* (Murrill) ascospore. The following properties were evaluated:

Stromata scattered, valsoid, yellow to yellowish-brown, brownish-red, prosenchymatous, up to 3 mm wide and 2.5 mm high.

Perithecia grouped, 15-30 in a stroma, more or less oblique, globose to depressed globose, 340-400 μm in diam., with dark brown to black, cylindrical, ostiolar beak, up to 900 μm long and 200 μm wide Asci paraphisatis, 8-spored, unitunicate, cylindrical-clavate, 30-50 $\times$ 6-9 μm.

Ascospores irregularly distichous, hyaline, 1-septate, constricted at the septum, elliptic, 5-12 $\times$ 3-5.5 μm. The identification of the fungus was conducted using the identification keys to compare the differences in shapes and sizes of spores, and the fact

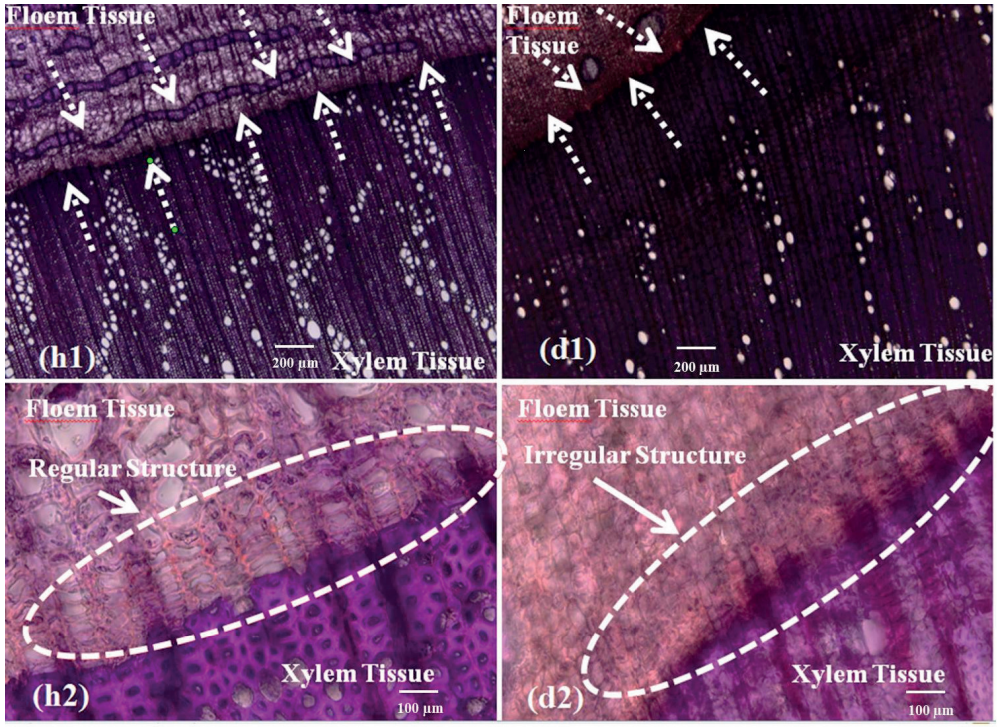

FIGURE 4 Light microscope images of CBD (d1, d2) and healthy (h1, h2) vascular cambium, secondary xylem, secondary phloem of chestnut.

that the microfungus was on a specific host plant also helped in the identification process.

Similar results were obtained in a study on CBD diseased wood, and *Cryphonectria parasitica* (Murrill) was found to be an ascomycete that utilizes wounds in the bark of chestnut trees to gain access and cause infection. The fungus grows in the bark of the tree, in characteristic fan-shaped mycelia, producing a canker on the tree. As the fungus grows, it colonizes the phloem and moves towards the vascular cambium and secondary xylem, destroying tissues as it progresses (GORDH; MCKIRDY, 2014).

To determine how it affects cellulose, hemicelluloses, and lignin, Raman analyses were performed on the cell wall of the vascular cambium, and the results are shown graphically in Figure10.

Raman Analysis

There are some differences in the FT-Raman band assignments, including the cellulose, hemicelluloses, and lignin of hardwoods, in the several reports that are summarized in Table 10 (AGARWAL et al., 1996; AGARWAL; KAWAI, 2003; ATALLA; AGARWAL, 1985; BARSBERG et al., 2005; FISCHER et al., 2005; LAVINE et al., 2001; LEWIS et al., 1994; PETROU et al., 2009).

FT-Raman band assignments for hardwoods can be summarized as follows: (EVANS, 1991; KENTON; RUBINOVITZ, 1990; OLDAK et al., 2005), the peak at 2907 cm^{-1} corresponds with cellulose and hemicellulose, and the shoulder at 2939 cm^{-1} relates to the presence of extractives and hemicellulose (Figure 10). The expected very intense peak with a shoulder at 1600 and 1660 cm^{-1} (LEWIS et al., 1994; ONA et al., 1997) are attributed to lignin. The phenol mode is expected at 1190 cm^{-1}, the lignin-carbohydrate complex has a peak at 1271 cm^{-1}, the cellulose peak at 1341 cm^{-1} and a very weak lignin and extractives peak located at 1297 cm^{-1} had also all disappeared. In the low frequency region of the Raman spectra of the hardwood samples, the shoulders on the cellulose peaks located at 353-380 and 436-459 cm^{-1} band level (GIERLINGER; SCHWANINGER, 2007). The hemicellulose peaks at 496-521 cm^{-1} also had shifted to 538 cm^{-1} and decreased in band intensity (PETROU et al., 2009).

According Table 10, similar peaks at the same point were found for both healthy and diseased samples; however, the intensities of the peaks of the healthy samples were determined to be lower than those of the diseased samples. In comparison with the healthy and diseased samples, it can be said that diseased samples appeared to have lost less carbohydrate and lignin than the healthy samples.

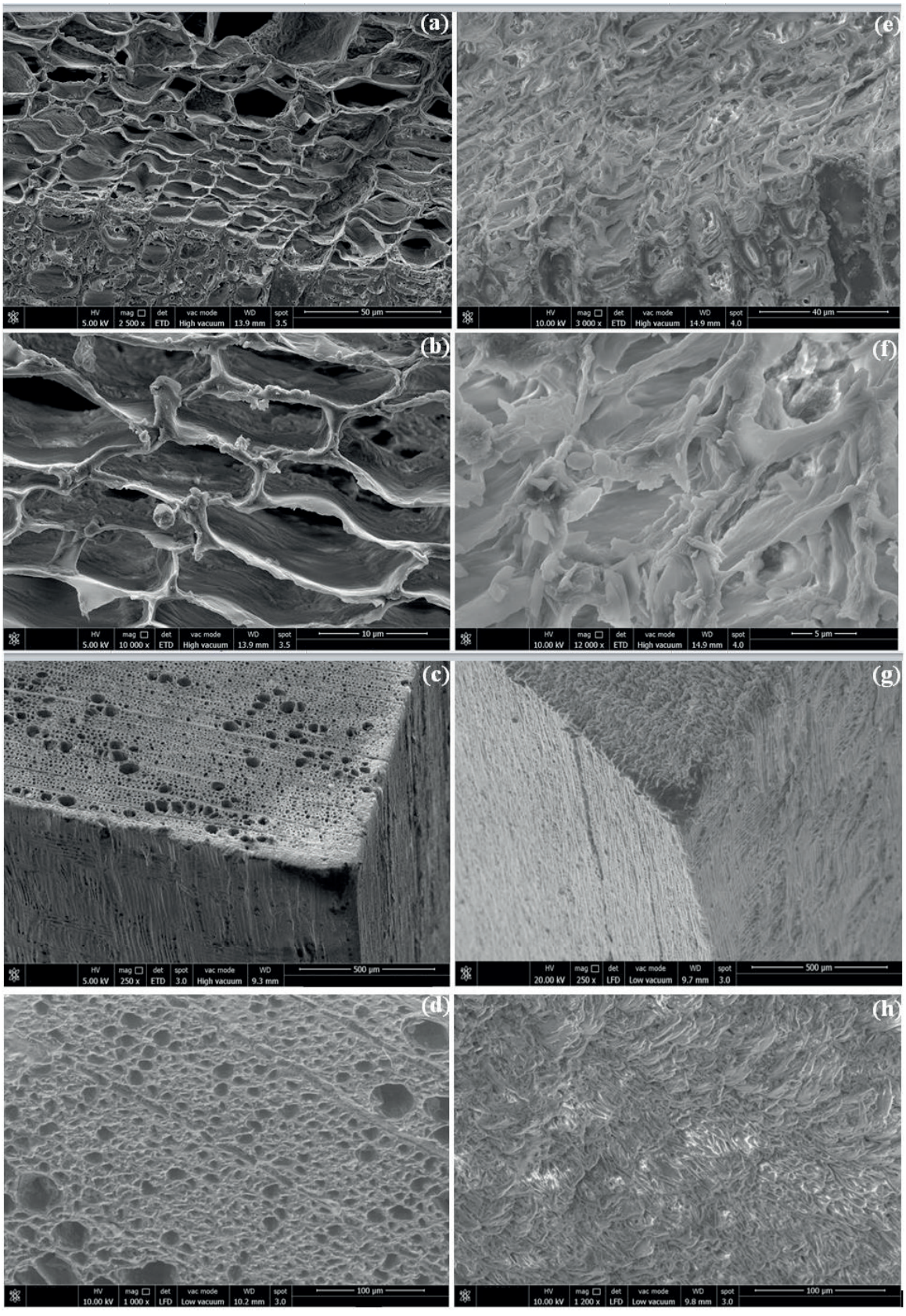

FIGURE 5 Healthy (a and b) and CBD diseased (e and f) chestnut cambium samples and healthy (c and d) and CBD diseased (g and h) wood samples.

TABLE 9 EDX analysis zones of cambium tissues belonging to the healthy (A) and diseased (B) wood.

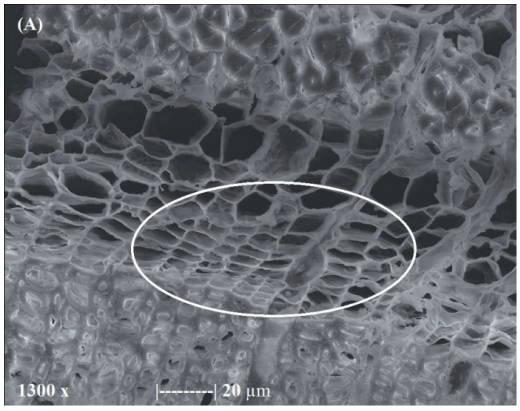

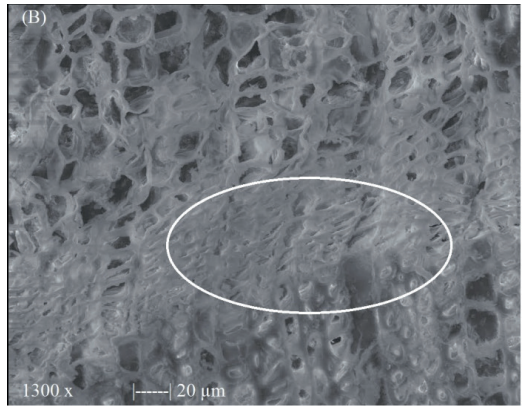

Element	(wt%)	(at%)	Element	(wt%)	(at%)
CK	69.22	75.05	CK	59.90	66.20
OK	30.48	24.81	OK	34.80	28.87
MgK	0.21	0.11	MgK	0.18	0.10
CaK	0.08	0.03	CaK	0.05	0.02
			NK	5.07	4.81

CONCLUSION

This is the first detailed study that has been conducted on *Cryphonectria parasitica* (Murrill) diseased Anatolian Chestnut trees. The SEM analysis showed that the cell structure changed in the vascular cambium and secondary xylem of the diseased tree. The cell structure was more irregular than in healthy trees. Due to its regional effect on the inner bark and vascular cambium, the diseased parts can be removed easily. The results

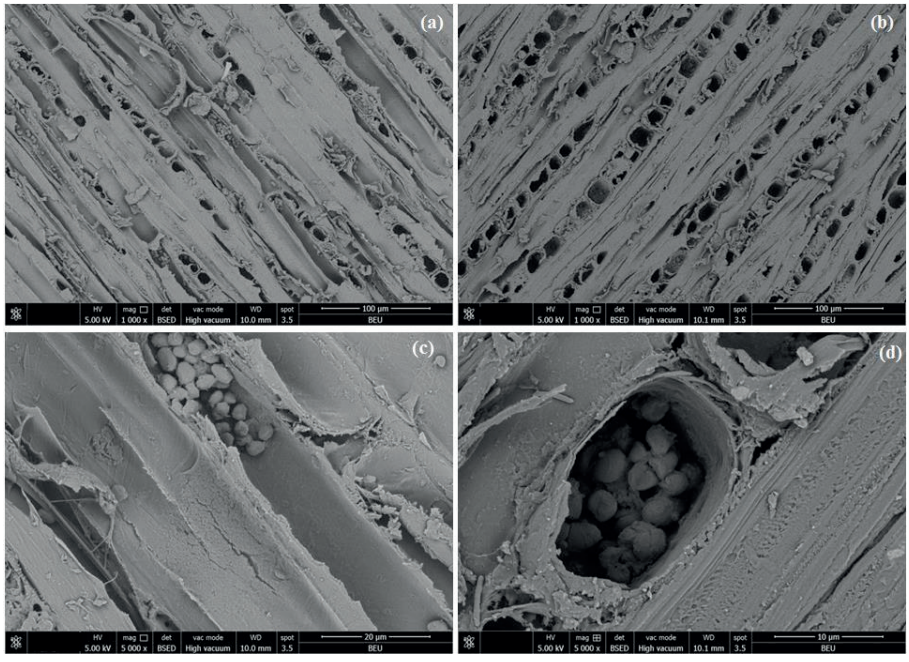

FIGURE 6 SEM images of the tangential sections of the diseased wood: starch grains in the ray parenchyma cells (a-b-d) and axial parenchyma cells (c).

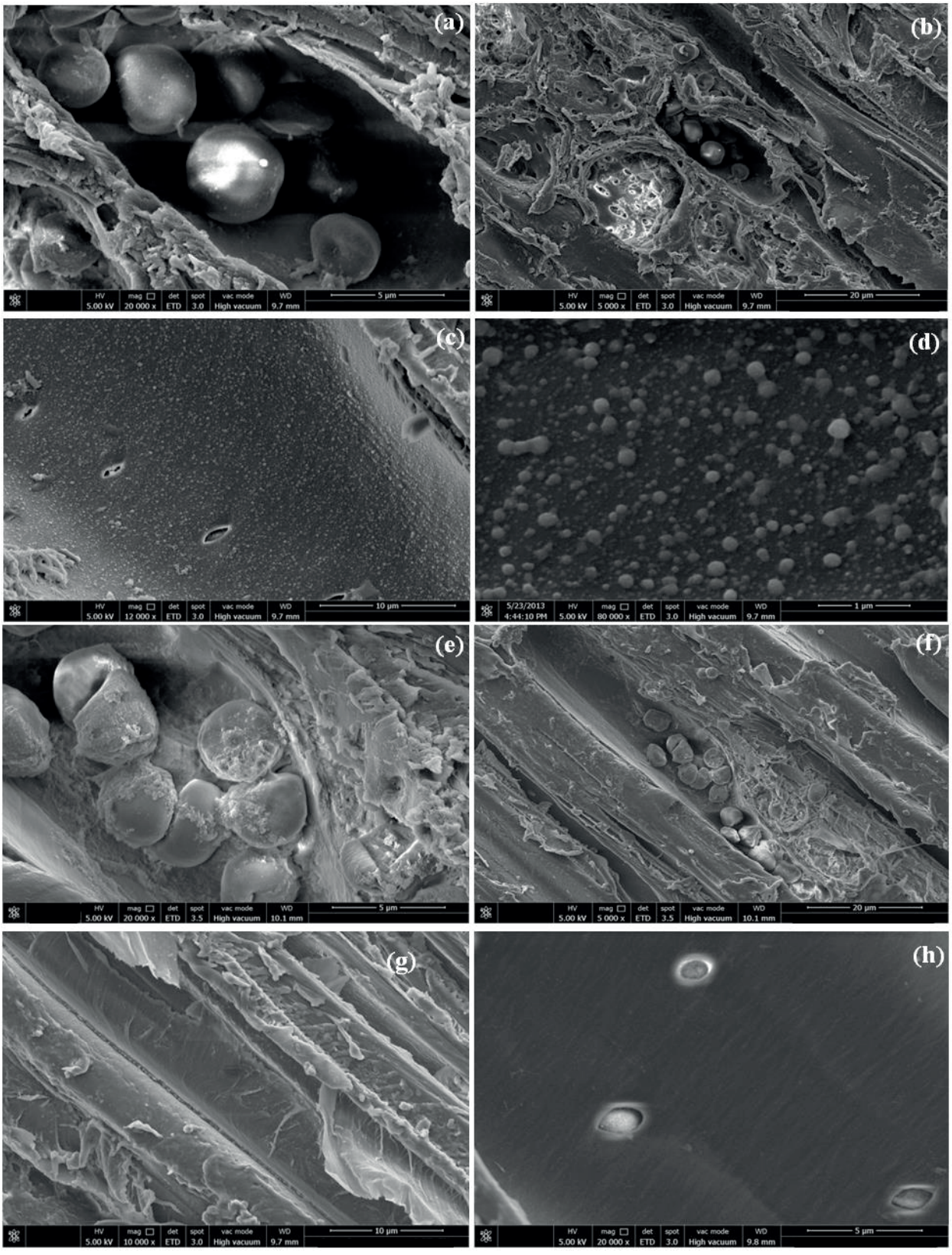

FIGURE 7 The SEM images of the starch grains in the parenchyma of the diseased (a and b) and healthy wood (e and f). Vessel inner cell wall surface in diseased (c and d) and healthy (g and h) wood.

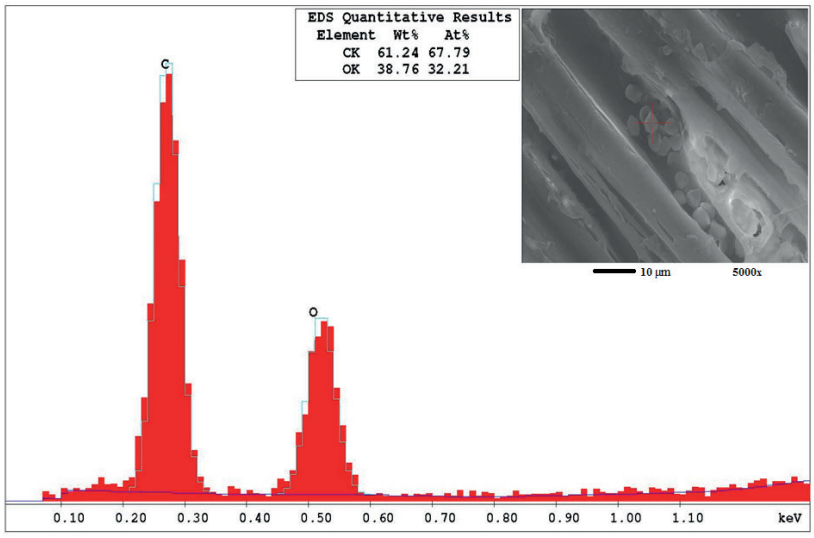

FIGURE 8 EDX analysis of the starch grains.

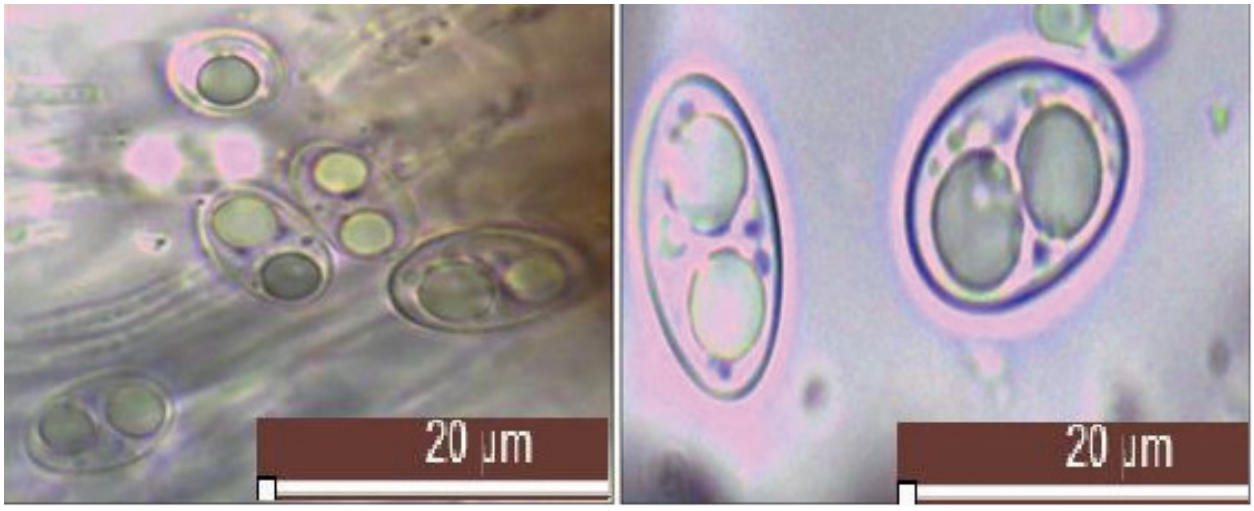

FIGURE 9 Analysis of the spores observed on the wood.

according to density and wood–water-related physical properties showed that the usability of the diseased chestnut wood is not limited. One way to prevent the spread of the disease in forests is to remove the diseased trees. These logs can be used in making furniture, shipbuilding, wooden building construction, and musical instruments. Heat treatment can be suggested for more dimensional stability and especially for sterilization of the timber obtained from the diseased trees. The physical properties, such as wood–water relations and density, did not change significantly. The yield of wood in diseased trees does not significantly decrease, and the wood can be used for quality timber production. The observation with unknown cause was that there was a granular appearance on the inner side of the vessels in the diseased zone. Generally, this warty layer develops during the last stages of cell differentiation and consists of the remnants of the protoplast (LIESE; LEDBETTER, 1963). Another difference between the diseased and healthy tissues of the wood was the increased percentage of elemental nitrogen in the diseased wood. This result confirmed that the CBD needed nitrogen. The Raman spectroscopic results showed a similar structure, but it can be said that the diseased samples appeared to have lost less carbohydrate and lignin than the healthy samples. The irregular cell structure of the vessels and fibers of the diseased wood showed some similarity with cancer in animals and humans.

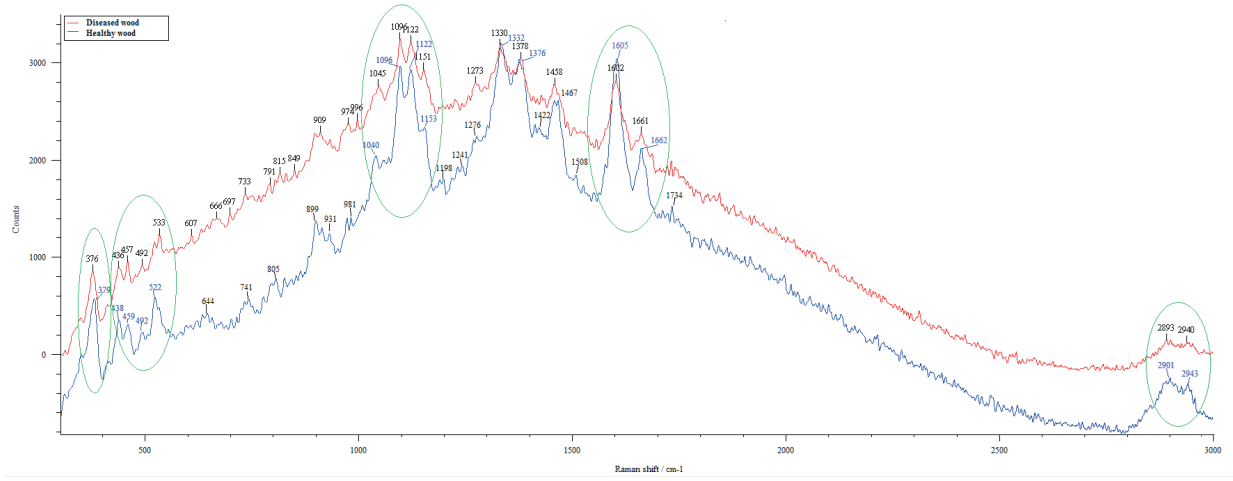

FIGURE 10 Cell wall analysis of healthy and diseased parts of vascular cambium using RS.

TABLE 10 FT-Raman band assignments for hardwoods reported in the literature (AGARWAL et al., 1996; AGARWAL; KAWAI, 2003; ATALLA; AGARWAL, 1985; BARSBERG et al., 2005; FISCHER et al., 2005; LAVINE et al., 2001; LEWIS et al., 1994; PETROU et al., 2009).

Band (cm^{-1})	Band Assignment	Band (cm^{-1})	Band Assignment
3020	Lignin	1119	Lignin and holocellulose
2939	Extractives hemicellulose	1118	Holocellulose
2907	Cellulose/hemicellulose	1093	Lignin
2900	Cellulose	1050	Lignin
1736	Holocellulose	1009	Cellulose
1379	Hemicellulose	897	Holocellulose
1377	Holocellulose	895	Crystalline and/or amorphous cellulose
1333	Holocellulose	524	Holocellulose
1327	Lignin	521	Hemicellulose
1318	Xylan	496	Hemicellulose
1312	Hemicellulose	459	Cellulose
1297	Lignin	436	Cellulose
1272	Rosin	380	Cellulose
1185	Holocellulose	376	Holocellulose
1180	Polystyrene butadiene	372	Holocellulose
1168	Cellulose		

ACKNOWLEDGEMENTS

We thank to the Forestry District in Bartin for kindly providing the plant material in this study. We also thank for Prof. Dr. Elsad Huseyin for his kindly contribution for analyzing the spores.

REFERENCES

AGARWAL, U. P.; ATALLA, R. H.; RALPH, S. A. Raman spectroscopy of lignin. In: ACS NATIONAL MEETING, 2011., 1996, New Orleans. **Abstracts...** New Orleans, ACS, 2011. 1 CD-ROM.

AGARWAL, U. P.; KAWAI, N. **FT-raman spectra of cellulose and lignocellulose materials:** "self-absorption" phenomenon and its implications for quantitative work. Madison: Forest Products Laboratory - USDA Forest Service, 2003.

ALLAHVERDIYEV, S. R.; KIRDAR, E.; GUNDUZ, G.; KADIMALIYEV, D.; REVIN, V.; FILONENKO, V.; RASULOVA, D. A.; ABBASOVA, Z. I.; GANI-ZADE, S. I.; ZEYNALOVA, E. Effective microorganisms (EM) technology in plants. **Technology**, v. 14, p. 103-106, 2011.

ANAGNOSTAKIS, S. L. American chestnut sprout survival with biological control of the chestnut blight fungus population. **Forest Ecology and Management**, v. 152, p. 225-233, 2001.

ANAGNOSTAKIS, S. L. Chestnut blight: the classical problem of an introduced pathogen. **Mycologia**, v. 79, p. 23-37, 1987.

ATALLA, R. H.; AGARWAL, U. Raman microprobe evidence for lignin orientation in the cell walls of native woody tissue. **Science**, New York, v. 227, p. 636-638, 1985.

BARAKAT, A.; STATON, M.; CHENG, C. H.; PARK, J.; YASSIN, N. B. M.; FICKLIN, S.; YEH, C. C.; HEBARD, F.; BAIER, K.; POWELL, W.; SCHUSTER, S.; WHEELER, N.; ABBOTT, A.; CARLSON, J. E.; SEDERO, R. Chestnut resistance to the blight disease: insights from transcriptome analysis. **BMC Plant Biology**, v 12, p. 1-14, 2012.

BARSBERG, S.; MATOUSEK, P.; TOWRIE, M. Structural analysis of lignin by resonance raman spectroscopy. **Macromolecular Bioscience**, v. 5, p. 743-752, 2005.

DAVIS, P. H. **Flora of turkey and east aegean Islands**. Edinburgh: Edinburgh University Press, 1982.

DOGU, D.; KOSE, C.; KARTAL, S. N.; ERDIN, N. Wood identification of wooden marine piles from the ancient byzantine port of eleutherius/Theodosius. **BioResources**, v. 6, p. 987-1018, 2011.

EVANS, P. A. Differentiating "hard" from "soft" woods using fourier transform infrared and fourier transform spectroscopy. **Spectrochimica Acta, Part A: Molecular and Biomolecular Spectroscopy**, v. 47, p. 1441-1447, 1991.

FISCHER, S.; SCHENZEL, K.; FISCHER, K.; DIEPENBROCK, W. Applications of FT raman spectroscopy and micro spectroscopy characterizing cellulose and cellulosic biomaterials. **Macromolecular Symposia**, v. 223, p. 41-56, 2005.

FOOD AND AGRICULTURE ORGANIZATION OF THE UNITED NATIONS. 2012. Available from: <http://faostat.fao.org/site/339/default.aspx>. Access in: 10 Dec. 2015.

FREINKEL, S. **American chestnut:** the life, death and rebirth of a perfect tree, Berkeley: University of California Press, 2007. 304 p.

GAERTNER, H.; SCHWEINGRUBER, F. H. **Microscopic preparation techniques for plant stem analysis**. Remagen: Verlag, 2013. 78 p.

GIERLINGER, N.; SCHWANNINGER, M. The potential of raman microscopy and raman imaging in plant research: review. **Spectroscopy**, v. 21, p. 69-89, 2007.

GORDH, G.; MCKIRDY, S. **The handbook of plant biosecurity**. New York: Springer, 2014.

GUNDUZ, G.; AYDEMIR, D.; ONAT, S. M.; AKGUN, K. The effects of tannin and thermal treatment on physical and mechanical properties of laminated chestnut wood composites. **BioResources**, v. 6, p. 1543-1555, 2011.

HAVIR, E.; ANAGNASTAKIS, S. L. Seasonal variation of peroxidase activity in chestnut trees. **Phytochemistry**, v. 48, p. 41-47, 1998.

INTERNATIONAL ASSOCIATION OF WOOD ANATOMISTS COMMITTEE. IAWA list of microscopic features for hardwood identification. **IAWA Bulletin**, v. 10, p. 219-332, 1989.

JACOBS, D. F. Toward development of silvical strategies for forest restoration of american chestnut (*Castanea dentata*) using blight-resistant hybrids. **Biological Conservation**, 137, p. 497-506, 2007.

KENTON, R. C.; RUBINOVITZ, R. L. FT-raman investigations of forest products. **Applied Spectroscopy**, v. 44, p. 1377-1380, 1990.

KIRK, P.; CANNON, P. F.; MINTER, D. W.; STALPERS, J. A. **Ainsworth & Bisby's dictionary of the Fungi**. 10th ed. Wallingford: CAB International, 2008.

LAVINE, B. K.; DAVIDSON, C. E.; MOORES, A. J.; GRIFFITHS, P. R. Raman spectroscopy and genetic algorithms for the classification of wood types. **Applied Spectroscopy**, v. 55, p. 960-966, 2001.

LEWIS, I. R.; CHAFFIN, N. C.; DANIEL, N. W.; GRIFFITHS, P. R. In: INTERNATIONAL CONFERENCE ON RAMAN SPEC, 14., 1994, Hong Kong. **Procedings…** Hong Kong, 1994.

LEWIS, I. R.; DANIEL, N. W.; CHAFFIN, J. N. C.; GRIFFITHS, P. R. Raman spectrometry and neural networks for the classification of wood types-1. **Spectrochimica Acta Part A: Molecular Spectroscopy**, v. 50, p. 1943-1958, 1994.

LIESE, W.; LEDBETTER, M. C. Occurrence of a warty layer in vascular cells of plants. **Nature**, London, v. 197, p. 201-202, 1963.

LOCCI, R. Chestnut blight: an epidemic checked by biological control. **Friulian Journal of Science**, v. 4, p. 27-45, 2003.

METAXAS, A. M. **Chestnut (*Castanea* spp.) cultivar evaluation for commercial chestnut production in hamilton county**. 2013. Dissertation (Master of Science in Environmental Science) - Faculty of the University of Tennessee, Tennessee, 2013.

MGM. Available from: <http://www.mgm.gov.tr/veridegerlendirme/il-ve-ilceler-istatistik.aspx?m=BARTIN>. 2014. Access in: 10 Dec. 2015.

MOLINARO, A.; LANZETTA, R.; MANCINO, A.; EVIDENTE, A.; DI ROSA, M.; IANARO, A. Immunostimulant (1→3)-D-glucans from the cell wall of *Cryphonectria parasitica* (Murr.) Barr strain 263. **Carbohydrate Research**, v. 329, p. 441-445, 2000.

OLDAK, D.; KACZMAREK, H.; BUFFETEAU, T.; SOURISSEAU, C. Photo- and bio-degradation processes in polyethylene, cellulose and their blends studied by ATR-FTIR and raman spectroscopies. **Journal of Materials Science**, v. 40, p. 4189-4198, 2005.

ONA, T.; SONODA, T.; SHIBATA, M.; KATO, T.; OOTAKE, Y. Non-destructive determination of wood constituents by fourier transform raman spectroscopy. **Journal of Wood Chemistry and Technology**, v. 17, p. 399-417, 1997.

PETROU, M.; EDWARDS, H. G. M.; JANAWAY, R. C.; THOMPSON, G. B.; WILSON, A. S. Fourier-transform raman spectroscopic study of a neolithic waterlogged wood assemblage. **Analytical and Bioanalytical Chemistry**, v. 395, p. 2131-2138, 2009.

ROBIN, C.; HEINIGER, U. Chestnut blight in europe: diversity of *Cryphonectria parasitica*, hypovirulence and biocontrol. **Forest Snow and Landscape Research**, v. 76, p. 361-367, 2001.

SCHAFLEITNER, R.; WILHELM, E. Effect of virulent and hypovirulent *Cryphonectria parasitica* (Murr.) Barr on the intercellular pathogen related proteins and on total protein pattern of chestnut (*Castanea sativa* Mill.). **Physiological and Molecular Plant Pathology**, v. 51, p. 323-332, 1997.

TULIK, M. Cambial history of Scots pine trees (*Pinus sylvestris*) prior and after the Chernobyl accident as encoded in the xylem. **Environmental and Experimental Botany**, v. 46, p. 1-10, 2001.

TURKISH STANDARTS. **TS 2471:** wood-determination of moisture content for physical and mechanical tests. Ankara, 1981a.

TURKISH STANDARTS. **TS 2472:** wood-determination of density for physical and mechanical tests. Ankara, 1985.

TURKISH STANDARTS. **TS 2483:** wood-determination of radial and tangential shrinkage. Ankara, 1983a.

TURKISH STANDARTS. **TS 4084:** wood-determination of radial and tangential swelling. Ankara, 1983b.

TURKISH STANDARTS. **TS 4085:** wood-determination of volumetric shrinkage. Ankara, 1983c.

TURKISH STANDARTS. **TS 4086:** wood-determination of volumetric swelling. Ankara, 1983d.

TURKISH STANDARTS. **TS 53:** wood-sampling and test methods-determination of physical properties. Ankara, 1981b.

VANNINI, A.; CARUSO, C.; LEONARDI, L.; RUGINI, E.; CHIAROT, E.; CAPORALE, C. Antifungal properties of chitinases from *Castanea sativa* against hypovirulent and virulent strains of the chestnut blight fungus *Cryphonectria parasitica*. **Physiological and Molecular Plant Pathology**, v. 55, p. 29-35, 1999.

WISE, L. E.; MAXINE, M.; D'ADDIECO, A. A. Chlorite holocellulose, its fractionation and bearing on summative wood analysis and studies on the hemicelluloses. **Paper Trade Journal**, v. 122, p. 35-43, 1946.

YAZICI, H. **Physical and mechanical properties of naturally curved growth (*Castanea sativa* Mill.) trees used for wooden ship building**. 1998. Thesis (Ph.D. in Forest Industrial Engineering) - Karaelmas University, Zonguldak, 1998.